

Acyl-coenzyme A organizes laterally in membranes and is recognized specifically by acyl-coenzyme A binding protein

A. Cohen Simonsen^{a,*}, U. Bernchou Jensen^a, N.J. Færgeman^b, J. Knudsen^b, O.G. Mouritsen^a

^aMEMPHYS, Physics Department, University of Southern Denmark, Campusvej 55, 5230 Odense M, Denmark

^bDepartment of Biochemistry and Molecular Biology, University of Southern Denmark, Campusvej 55, 5230 Odense M, Denmark

Received 16 July 2003; revised 25 August 2003; accepted 26 August 2003

First published online 8 September 2003

Edited by Amy McGough

Abstract Long chain acyl-coenzyme A (acyl-CoA) is a biochemically important amphiphilic molecule that is known to partition strongly into membranes by insertion of the acyl chain. At present, microscopically resolved evidence is lacking on how acyl-CoA influences and organizes laterally in membranes. By atomic force microscopy (AFM) imaging of membranes exposed to acyl-CoA in μM concentrations, it is shown that aggregate formation takes place within the membrane upon long-time exposure. It is known that acyl-CoA is bound by acyl-CoA binding protein (ACBP) with high affinity and specificity and that ACBP may bind and desorb membrane-bound acyl-CoA via a partly unknown mechanism. Following incubation with acyl-CoA, it is shown that ACBP is able to reverse the formation of acyl-CoA aggregates and to associate peripherally with acyl-CoA on the membrane surface. Our microscopic results point to the role of ACBP as an intermembrane transporter of acyl-CoA and demonstrate the ability of AFM to reveal the remodelling of membranes by surfactants and proteins.

© 2003 Published by Elsevier B.V. on behalf of the Federation of European Biochemical Societies.

Key words: Lipid bilayer membrane; Atomic force microscopy; Long chain fatty acyl-coenzyme A; Acyl-coenzyme A binding protein; Phosphatidylcholine

1. Introduction

The lipid bilayer is the essential structural component of biological membranes and for biophysical studies, supported or free-standing lipid bilayers are often utilized as well-controlled model systems for biological cell membranes. An important class of phenomena is the interaction of membranes with amphiphilic surfactants present in the water phase, and long chain fatty acyl-coenzyme A thioesters (LCFA-CoA) exemplify a biochemically important surfactant. LCFA-CoAs are activated derivatives of fatty acids that serve as intermediates in lipid metabolism and lipid biosynthesis, and have also been reported to influence a wide range of membrane-bound proteins and cellular functions [1] such as ion pumps, ion channels and enzymes, membrane budding and fusion events [2–4] as well as gene expression [5]. LCFA-CoA molecules are amphiphilic molecules with a hydrophobic fatty acid chain and a polar, hydrophilic CoA head group. The critical micellar concentration (CMC) of palmitoyl-CoA

was found [6–8] to vary with salt concentration and pH, but with a typical value around 30–40 μM .

LCFA-CoAs are known to associate with phospholipid membranes by insertion of the fatty acyl chain [9,10] into the bilayer core. In this respect, acyl-coenzymes A (acyl-CoAs) may be classified together with other membrane associating surfactants such as lysolipids, acylated peptides or acyl-carnitines [11,12], of which the latter occur in metabolism along with acyl-CoA. The equilibrium partitioning of acyl-CoA into membranes is described by the partition constant K_p which is the ratio between the mole fraction χ of surfactant in the membrane and the aqueous molar concentration c (M) of surfactant in the water phase. For palmitoyl-CoA (C_{16} -CoA) in equilibrium with phospholipid vesicles, K_p is typically of the order of $1 \times 10^5 \text{ M}^{-1}$ [10,13].

Acyl-CoA is also the ligand of acyl-CoA binding protein (ACBP), a cytosolic protein, mass = 10 kDa, that binds C_{14} – C_{22} acyl-CoA with high affinity (K_D is typically of the order of 0.1 nM) and specificity [14,15]. ACBP has been found in all eukaryotes tested and is believed to function as a pool former and transporter for acyl-CoA. ACBP has been found to mediate the intermembrane transport of LCFA-CoAs and to donate LCFA-CoAs to β -oxidation in mitochondria [16].

The membrane partitioning of LCFA-CoAs has previously been studied to some extent by measurements of vesicle suspensions. Nuclear magnetic resonance (NMR) shows no transbilayer movement of oleoyl-CoA in egg-PC vesicles [9] and the membrane affinity was higher than for octanoyl-CoA. Palmitoyl-CoA has been reported to permeabilize rat liver microsomal vesicles [17], whereas other studies did not find solubilization or leakage of egg-PC vesicles by palmitoyl-CoA [11]. In contrast, acyl-carnitines have been found to yield membrane solubilization analogous to what is induced by synthetic surfactants [12]. Regarding thermodynamic properties, C_{14} -CoA has been found by differential scanning calorimetry to increase the width of the main gel–fluid phase transition in saturated phosphatidylcholines [18].

In view of the sparse available knowledge of the microscopic details for LCFA-CoA/membrane interactions it appears highly relevant to characterize with high spatial resolution, how well-defined membranes are influenced by the partitioning of LCFA-CoA. By atomic force microscopy (AFM) we study the morphological changes that occur in supported membranes after exposure to acyl-CoA and we investigate whether these changes can be reversed by subsequent exposure to ACBP and whether ACBP binds to the membrane. In an attempt to establish the basic phenomenology pertaining to these problems, we use a model membrane system with the

*Corresponding author. Fax: (45)-6615-8760.

E-mail address: adam@memphys.sdu.dk (A. Cohen Simonsen).

lowest complexity, which in this case means one-component fluid bilayer membranes of DOPC (1,2-dioleoyl-*sn*-glycero-3-phosphocholine).

2. Materials and methods

DOPC was purchased from Avanti Polar Lipids Inc. Acyl-CoA was synthesized from CoA and fatty acid as described in [19]. ACBP (bovine) was expressed in *Escherichia coli* and purified as described in [20]. Fatty acid free bovine serum albumine (BSA) was purchased in powder form from Sigma-Aldrich. Supported lipid bilayers of DOPC were prepared by Langmuir–Blodgett (LB) deposition using a monolayer trough (μ -trough, Kibron Inc.) and Milli-Q water as subphase. Freshly cleaved mica sheets were used as solid supports. Lipid was applied to the water surface from a lipid stock solution of 0.5 mg/ml (DOPC in hexane) and solvent evaporation was allowed for 30 min. The monolayer was compressed at $2 \text{ \AA}^2/\text{chain}/\text{min}$ to a final pressure of 42 mN/m, and the monolayer was transferred to mica with a vertical dipping speed of 1–3 mm/s and with a subphase temperature maintained at $T = 20.0^\circ\text{C}$. Two vertical depositions of monolayers produced a supported lipid bilayer membrane and the sample was thereafter transferred to the AFM liquid cell without exposure to air. AFM measurements were performed with a PicoSPM atomic force microscope (Molecular Imaging) equipped with a home-made liquid cell and operated in magnetically driven tapping mode (MAC-mode) using MAClevers supplied by Molecular Imaging and with a resonance frequency in water of $\sim 30 \text{ kHz}$. AFM was carried out at room temperature ($\sim 20^\circ\text{C}$). The scanner was continuously moved to new regions during experiments with acyl-CoA and ACBP. This is necessary due to the fact that the interaction of the membrane with molecules in the water phase is sensitive to cantilever motion and tip–surface contact. Moreover, it is not feasible to keep the sample in the AFM and to keep the scanner at a fixed position over the long periods involved in the present experiment. Despite the fact that this procedure eliminates the option of following local changes in the membrane, it secures a reliable characterization of the true and unperturbed morphology. In addition, the samples were in all cases found to be quite uniform, meaning that a given region is representative for the appearance of the complete sample. Note, that when imaging structures that are comparable to or smaller than the apex of the AFM tip (20–50 nm), the spatial resolution will be affected by broadening [21]. For well-separated structures protruding from a planar surface, this effect will typically imply that the recorded width is too large, whereas the height of the structures is recorded accurately.

Acyl-CoA solutions were injected directly into the fluid cell via Teflon tubing and the aqueous cell volume was exchanged by flushing within 20–30 s. ACBP was subsequently injected into the cell in concentrated form from a stock solution of 3–4 mg/ml in order to minimize the effect of diluting the LCFA-CoA already present in the cell.

3. Results

Fig. 1A,D shows the typical appearance of a native DOPC membrane as formed by LB deposition. These membranes usually contain well-defined holes in the range of 5–10% of the surface area. The difference in height between hole and membrane regions was in the range of 15–35 Å. The height of the deepest holes correspond to the reported thickness of a fluid DOPC bilayer of 35 Å [22]. In general, it was found that the interaction of the supported membranes with acyl-CoA can be divided in two stages: The initial partitioning of C_{18} -CoA into the membrane occurs within seconds after exposure (flushing of the liquid cell) and this is followed by a much slower second stage involving lateral diffusion of LCFA-CoA. The initial stage is characterized by a strong disturbance of the membrane surface and was found to be difficult to image with AFM. In the second stage, stabilization of the surface topology and formation of elevated structures occurs after

incubation with acyl-CoA for 5–10 h. These structures are assumed to be enriched in acyl-CoA and for convenience they are termed aggregates. The nature and composition of the structures are discussed further below. Fig. 1B shows the aggregates formed after incubation for 15 h with $5 \text{ }\mu\text{M}$ C_{18} -CoA. Aggregates have a typical height of 20–40 Å and are preferentially located at hole edges. This is consistent with previous findings that a high membrane curvature at hole edges will favor the accommodation of molecules with more bulky head groups [23,24]. Note that aggregates are also found in the homogeneous parts of the membrane with no holes, indicating that the aggregation process itself is not confined to hole edges. Likewise, analogous experiments on hole free membranes also produce aggregates. The aggregates found in uniform membrane regions have poorly defined shapes and are more susceptible to scanner-induced motion, probably because they are not pinned.

Fig. 1C shows the sample in Fig. 1B after 30 min exposure to an excess amount of ACBP (1.5 times the equivalent to C_{18} -CoA). At this point, the acyl-CoA aggregates have been nearly completely removed from the membrane and only a few aggregates are seen. This means that in the process where ACBP binds to the acyl-CoA or to the CoA head group, the membrane partitioning and formation of aggregates is reversed. The stripes observed in Fig. 1C show the appearance of acyl-CoA aggregates that are being moved by the tip during scanning and demonstrate the high lateral mobility of the aggregates.

For DOPC membranes exposed to $10 \text{ }\mu\text{M}$ C_{18} -CoA it is found that larger aggregates are formed compared to the $5 \text{ }\mu\text{M}$ case. Membrane solubilization induced by acyl-CoA was not observed even at $10 \text{ }\mu\text{M}$. After exposure of the initial membrane in Fig. 1D to acyl-CoA, a period of membrane destabilization is once again observed. After overnight incubation of the membrane, aggregates around holes are observed, as in Fig. 1E. In this case, the acyl-CoA may aggregate into highly compact structures around holes to an extent where only a few narrow channels remain in the central part of the aggregate region. Since the edges of holes possess a high degree of curvature that accommodates acyl-CoA, one might speculate that the complete sealing of holes is unfavorable since it would force the surface to become less curved at this point. The aggregates protrude 20–30 Å above the membrane surface and do not possess regular boundaries or surface shapes. Rather the surface morphology is corrugated or amorphous, as revealed by the close-up in Fig. 1F. This suggests that the acyl-CoA favors a membrane interface with high curvature and that a dense population of acyl-CoA is not compatible with a planar membrane surface.

After exposure of the membrane in Fig. 1E,F to 1.5 times the equivalent amount of ACBP, the structures in Fig. 1G,H were observed within minutes thereafter. It is found that the acyl-CoA aggregates of Fig. 1E,F have disappeared, and that the holes in the membrane have re-emerged (regions marked with crosses in Fig. 1G). The membrane holes are now covered with an ACBP monolayer due to the interaction with the mica substrate, as described below in Section 3.1. Furthermore, for the membranes that were exposed to $10 \text{ }\mu\text{M}$ C_{18} -CoA, a pattern is observed on the membrane which is interpreted as ACBP associated peripherally with the membrane surface. The ACBP is bound to the membrane in clusters with a lateral size of a few hundred nanometers. The height of the

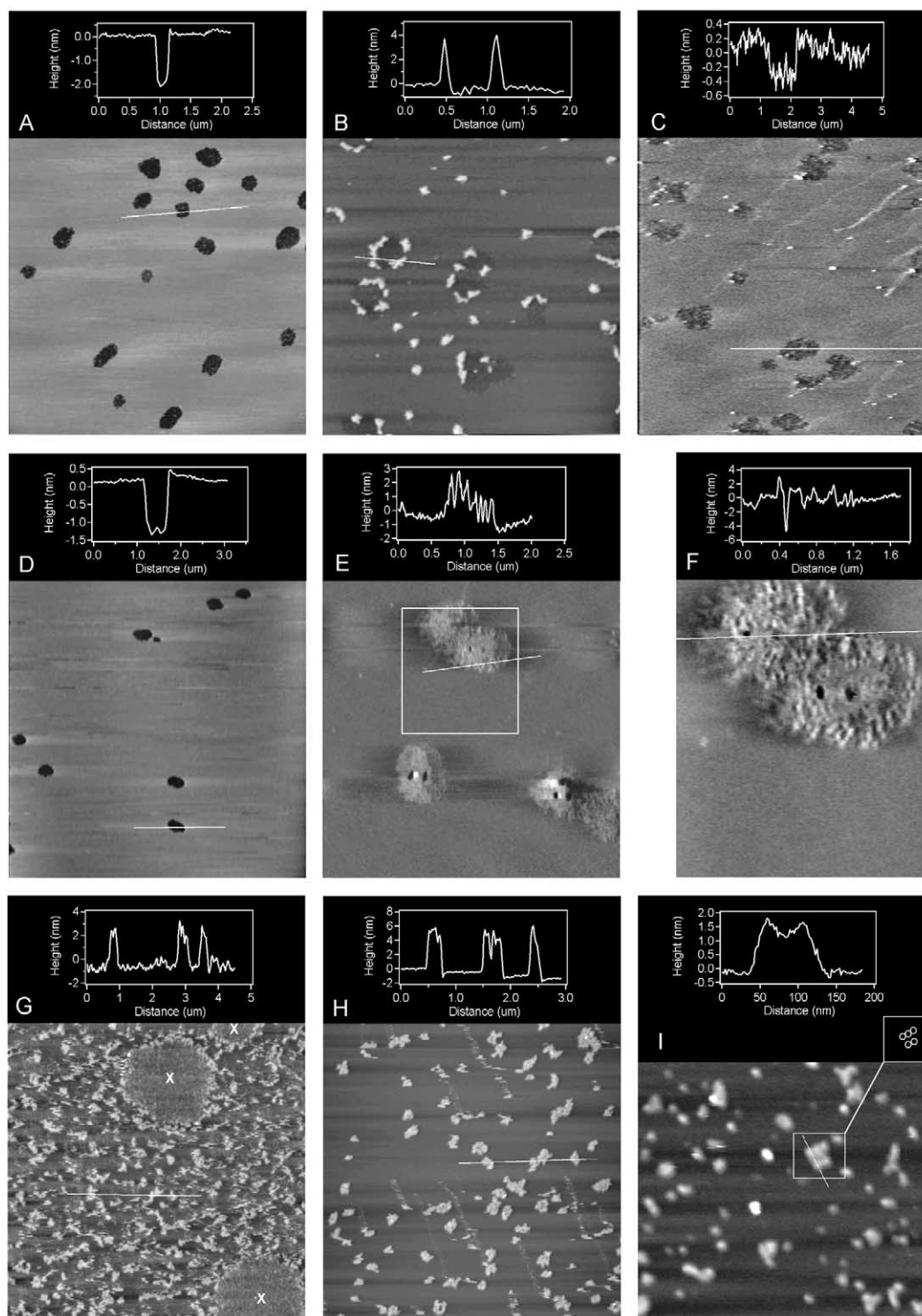


Fig. 1. The effect of acyl-CoA and ACBP on membrane topology. All images are accompanied by a height profile corresponding to the line indicated in the image. The bare DOPC membrane in A is planar and featureless except for some holes extending partly down to the support surface. Upon exposure of the membrane to 5 μM C₁₈-CoA for 15 h, stable acyl-CoA aggregates are formed preferentially at hole edges (B). After exposing this membrane to 1.5 times the equivalent ACBP dose, the acyl-CoA aggregates have been almost completely removed after 30 min (C). Upon exposure of the membrane in D to an increased 10 μM concentration of C₁₈-CoA, larger acyl-CoA aggregates develop (E). The corrugated topology of the aggregate regions is shown more detailed in the close-up (F). Exposing the membrane in E, F to 1.5 times the equivalent ACBP dose, the acyl-CoA aggregates are removed and clusters of membrane-associated ACBP are observed on the membrane surface (G, H, I). The close-up in I shows a region with ACBP clusters consisting of repeated subunits that are indicative of single proteins.

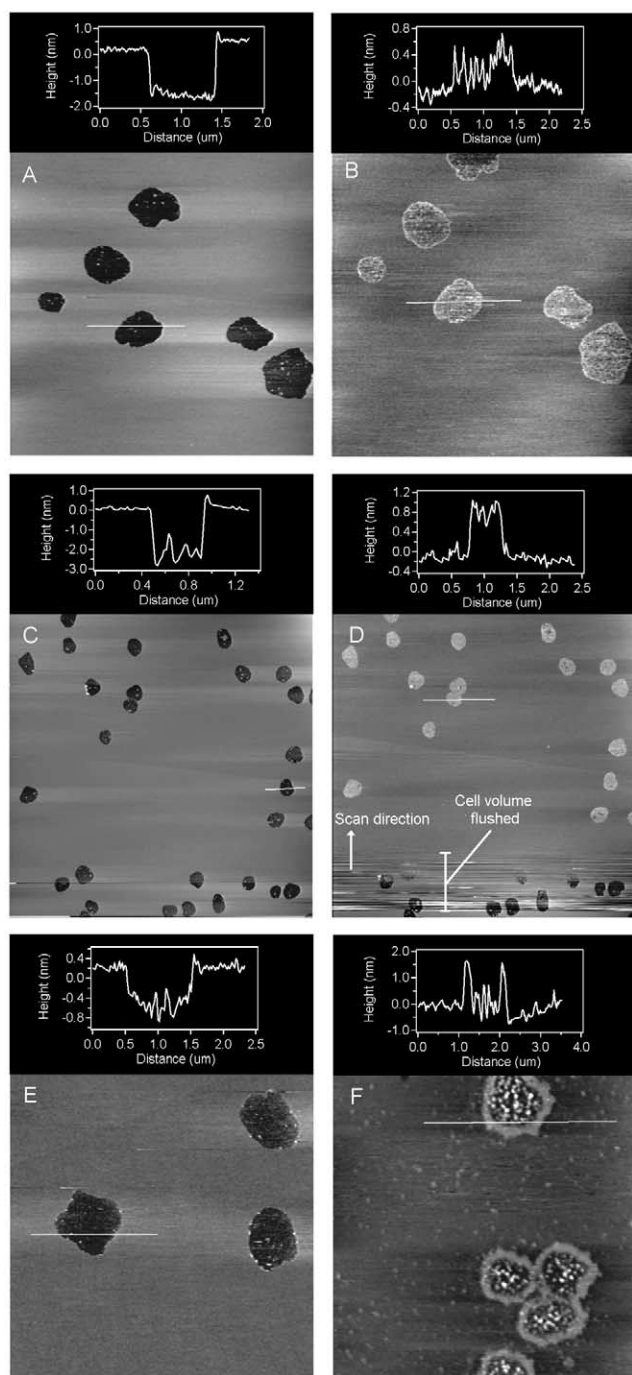


Fig. 2. Control experiments carried out to verify the specificity of the membrane interactions and the unspecific adsorption to holes, seen in Fig. 1. The unexposed DOPC membranes are shown for reference in A, C, E and they are featureless except for some well-defined hole regions. When the membrane region in A is exposed to 5 μM ACBP, holes in the same region are covered with a monolayer of protein adsorbed to the mica surface, while there are no visible changes in the membrane topology (B). Similarly, the membrane in C was exposed to the protein/ligand complex (20 μM ACBP+10 μM $\text{C}_{18}\text{-CoA}$) and the point at which the complex was injected into the fluid cell is indicated in D. Proteins again adsorb unspecifically to the holes, but the protein/ligand complex does not bind to the membrane surface. The specificity of ACBP towards membrane-bound acyl-CoA was checked in E, F by using BSA. The membrane in E was exposed overnight to 10 μM $\text{C}_{18}\text{-CoA}$ followed by 1.5 times the equivalent BSA dose (F). In this case, acyl-CoA aggregates are still present at the hole edges, and BSA does not bind to the membrane surface.

ACBP regions is 2–4 nm, in fair agreement with the reported size of the ACBP molecule ($21 \times 31 \times 38 \text{ \AA}$) [16,25] and suggesting that stacking of the protein does not occur. Fig. 1I shows a region for which the structure of the membrane-associated ACBP is more clearly resolved. In this image, the ACBP regions appear to consist of subunits that all have nearly the same size (see the square indicated in Fig. 1I). The height and the uniform size of the subunits are indicative of single ACBP proteins bound to the membrane. The lateral size of the proteins is exaggerated due to the influence of the tip shape on the measured topology.

3.1. Control experiments

Both LCFA-CoA and ACBP are charged molecules and it is therefore important to rule out the possibility that membrane binding of ACBP is simply due to electrostatic interactions with the membrane and/or with the mica support. Additionally we would like to verify the specificity of the membrane association of ACBP using BSA as a control protein. The following control experiments were carried out to address these issues. Fig. 2A,C,E shows DOPC bilayer membranes as formed. A few minutes after exposing the membrane in Fig. 2A to 5 μM ACBP, a strong interaction with the mica substrate within the holes can be observed (Fig. 2B). More importantly there are no detectable changes in the uniform membrane regions after ACBP exposure, indicating that the protein does not bind to planar DOPC membranes in the absence of LCFA-CoA. The exposed mica surface within the holes becomes covered with a monolayer of ACBP molecules. This is evident from the change in topographical height of the hole regions after exposure to ACBP which corresponds roughly to the dimensions of the ACBP molecule. The adsorption of proteins to mica in aqueous environment is well known and has been used for immobilization purposes in several studies [26–28]. An experiment where pure mica was exposed to ACBP showed surface binding of ACBP also in the absence of a membrane.

Since the ACBP–ligand complex has a different charge state than the ACBP itself, it is also important to clarify whether the membrane binding observed in Fig. 1G,H,I is due to an electrostatic interaction between the ACBP–ligand complex and the membrane. Fig. 2C,D shows a control experiment where a DOPC membrane has been exposed to the ACBP–ligand complex (20 μM ACBP+10 μM $\text{C}_{18}\text{-CoA}$). The result shows again a strong affinity of the protein to the mica substrate, while there is no detectable membrane binding of the protein or the complex to the membrane surface. Fig. 2D shows the point at which the cell volume is exchanged with acyl-CoA/ACBP solution and that holes that are scanned after this event are saturated with protein. These control experiments support the conclusion that the membrane binding of ACBP observed in Fig. 1G,H is mediated by the presence of acyl-CoA in the membrane and is not caused by interactions between the membrane and ACBP or the ACBP–ligand complex. It is found that ACBP associates with the mica support, but this binding is confined to holes where the mica is exposed.

The specificity of ACBP towards acyl-CoA partitioned into the membrane was checked using BSA as a control. BSA is known to bind acyl-CoA with an affinity of 2 μM (N.J. Færgeman and J. Knudsen, unpublished results) and it is unable to fully extract membrane-bound acyl-CoA. Fig. 2F

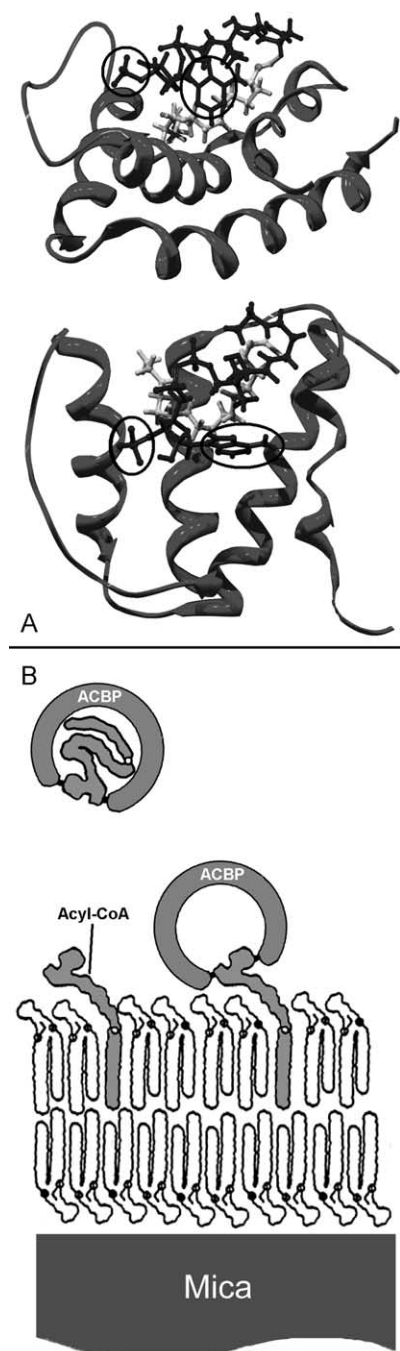


Fig. 3. Structural 3D model (A) of ACBP in complex with C_{16} -CoA, based on NMR data [25] (CoA group=dark, acyl chain=bright). The CoA head group has strong and specific interactions with ACBP at the 3' phosphate and at the adenine group (encased regions in A). The acyl chain is shielded from the solvent phase and interacts hydrophobically with the ACBP core. Schematic drawing of a possible structural mechanism for the recognition and binding of ACBP to membrane-associated acyl-CoA (B).

shows the membrane in Fig. 2E exposed to $10\ \mu\text{M}$ C_{18} -CoA followed by exposure to 1.5 times the equivalent BSA dose. All edges of the holes in the membrane are saturated with acyl-CoA aggregates and the BSA treatment have not resulted in removal of the aggregates, nor do we observe any association of BSA to the membrane.

4. Discussion

Based on the present AFM experiments we conclude that the interaction of a DOPC membrane with C_{18} -CoA occurs in two stages, the first involves partitioning of acyl-CoA from the water phase into the membrane and occurs in seconds or less after exposure. AFM imaging of this stage is difficult, probably because the membrane surface is highly dynamic during acyl-CoA uptake, and changes in the membrane occur faster than the time required to obtain an image. Going into the second stage after several hours, lateral diffusion leads to the formation of structures that are 2–4 nm high and preferentially pinned to hole edges. These aggregated structures are generated by the presence of acyl-CoA in the membrane. Their molecular composition cannot be inferred directly from AFM. However, for membranes exposed to acyl-CoA, a subsequent exposure to ACBP in excess leads to removal of the aggregates within minutes suggesting that the aggregates are mainly composed of acyl-CoA. Since we use acyl-CoA concentrations that are about 5 times below the CMC, it seems highly unlikely that the aggregates are simply adsorbed micelles. The height of the aggregates is somewhat larger than what would be expected in the case of CoA groups that are protruding from a planar bilayer. Rather, it is possible that the structure of the aggregates is that of a mixed DOPC/acyl-CoA phase. Considering the corrugated topology of the aggregate in Fig. 1F, this phase might be a strongly perturbed bilayer structure or even a non-bilayer phase. Acyl-CoA residing in the membrane is only detected to the extent that it gives rise to variations in the surface topography or mechanical response. Indeed we can conclude from the uniform binding of ACBP to the entire membrane, that aggregates do not account for all of the membrane-associated acyl-CoA. It is an open question whether the aggregation is different for free-standing membranes, and whether the formation of aggregates is targeted toward specific functions in live cells.

Pre-exposure to $10\ \mu\text{M}$ C_{18} -CoA leads to the peripheral binding of ACBP molecules to the membrane. A much lower density of ACBP clusters is observed on membranes exposed to $5\ \mu\text{M}$ C_{18} -CoA. While the height of the clusters matches the dimensions of an ACBP molecule, the lateral width is enhanced due to the broadening effect of the AFM tip. The actual number of ACBP molecules bound to the membrane could therefore be quite small compared to an estimate based only on the measured width of the clusters.

By control experiments it is established that the membrane association of ACBP is mediated by the pre-exposure to acyl-CoA and not due to an electrostatic or other unspecific attraction. The specificity of ACBP towards membrane-bound acyl-CoA was verified using BSA as a control protein. In view of our results, it is interesting that binding of ACBP to highly curved, anionic membranes has recently been reported [29]. This interaction, however, correlated with the charge of the ligand protein complex indicating that the observed interaction in this case is electrostatically driven.

The three-dimensional (3D) structure of the complex between C_{16} -CoA and ACBP has been solved [25] and is shown in Fig. 3A. The structural investigations have shown that ACBP has strong and specific interaction with the CoA head group at the 3' phosphate (accounts for 40% of the binding energy) and the adenine positions. In addition, a hydrophobic attraction exists between the acyl chain and the

ACBP core. It was shown previously that ACBP binds to the pure CoA with a K_D of 2 μ M [30]. If ACBP has access to the CoA group of membrane-bound LCFA-CoA, a specific recognition and binding of the CoA group only, could take place as sketched in Fig. 3B. There is a correlation between the concentration of acyl-CoA and the density of ACBP that subsequently binds to the membrane. This indicates that with a dense population of acyl-CoA embedded in the membrane, ACBP associates to the CoA group without extracting the acyl-CoA molecule from the membrane. This could be due to enhanced attractive interactions between acyl-CoA molecules at high concentrations, resulting in a denser packing and stronger anchoring of the acyl chain to the membrane.

Taken together, our results suggest that ACBP is able to extract LCFA-CoA molecules from membranes by direct interaction and binding to LCFA-CoA molecules embedded in the membrane. Evidence has previously been presented [29,16] which implicates such a mechanism to be associated with the action of ACBP in intermembrane transport and the present study has provided some further microscopic evidence for this mechanism. Our approach demonstrates the ability of AFM to follow changes in a membrane which is perturbed by a surfactant molecule and remodelled by the action of a specific binding protein.

Acknowledgements: A.C.S., U.B.J. and O.G.M. are grateful to the Danish National Research Foundation for support via a grant to the MEMPHYS-Center for Biomembrane Physics.

References

- [1] Færgeman, N.J. and Knudsen, J. (1997) *Biochem. J.* 323, 1–12.
- [2] Glick, B.S. and Rothman, J.E. (1987) *Nature* 326, 309–312.
- [3] Pfanner, N., Orci, L., Glick, B.S., Amherdt, M., Arden, S.R., Malhotra, V. and Rothman, J.E. (1989) *Cell* 59, 95–102.
- [4] Pfanner, N., Glick, B.S., Arden, S.R. and Rothman, J.E. (1990) *J. Cell Biol.* 110, 955–961.
- [5] Hertz, R., Magenheimer, J., Berman, I. and Bar-Tana, J. (1998) *Nature* 392, 512.
- [6] Requero, M.A., Goni, F.M. and Alonso, A. (1993) *J. Colloid Interface Sci.* 161, 343–346.
- [7] Requero, M.A., Goni, F.M. and Alonso, A. (1996) *J. Colloid Interface Sci.* 177, 681.
- [8] Das, A.K. and Hajra, A.K. (1992) *J. Biol. Chem.* 267, 9731.
- [9] Boylan, J.G. and Hamilton, J.A. (1992) *Biochemistry* 31, 557–567.
- [10] Pitzsh, R.M. and McLaughlin, S. (1993) *Biochemistry* 32, 10436–10443.
- [11] Requero, M.A., Goni, F.M. and Alonso, A. (1995) *Biochemistry* 34, 10400–10405.
- [12] Goni, F.M., Requero, M.A. and Alonso, A. (1996) *FEBS Lett.* 390, 1–5.
- [13] Requero, M.A., Gonzalez, M., Goni, F.M., Alonso, A. and Fidelio, G. (1995) *FEBS Lett.* 357, 75–78.
- [14] Mogensen, I.B., Schulenberg, H., Hansen, H.O. and Knudsen, F.S.J. (1987) *Biochem. J.* 241, 189.
- [15] Kragelund, B.B., Knudsen, J. and Poulsen, F.M. (1999) *Biochim. Biophys. Acta* 1441, 150–161.
- [16] Rasmussen, J.T., Færgeman, N.J., Kristiansen, K. and Knudsen, J. (1994) *Biochem. J.* 299, 165–170.
- [17] Banhegyi, G., Csala, M., Mandl, J., Burchell, A., Burchell, B., Amcolongo, P., Fulceri, R. and Benedetti, A. (1996) *Biochem. J. Lett.* 320, 343–344.
- [18] Veiga, M.P., Requero, M.A., Goni, F.M. and Alonso, A. (1996) *Mol. Membr. Biol.* 13, 165–172.
- [19] Rosendal, J., Ertbjerg, P. and Knudsen, J. (1993) *Biochem. J.* 290, 321–326.
- [20] Mandrup, S., Højrup, P., Kristiansen, K. and Knudsen, J. (1991) *Biochem. J.* 276, 817–823.
- [21] Villarrubia, J.S. (1997) *J. Res. Natl. Inst. Stan.* 102, 425–454.
- [22] Costigan, S.C., Booth, P.J. and Templer, R.H. (2000) *Biochim. Biophys. Acta* 1468, 41–54.
- [23] Grandbois, M., Clausen-Schaumann, H. and Gaub, H. (1998) *Biophys. J.* 74, 2398–2404.
- [24] Kaasgaard, T., Mouritsen, O.G. and Jørgensen, K. (2002) *FEBS Lett.* 515, 29–34.
- [25] Kragelund, B.B., Andersen, K.V., Madsen, J.C., Knudsen, J. and Poulsen, F.M. (1993) *J. Mol. Biol.* 230, 1260–1277.
- [26] Yang, J., Mou, J. and Shao, Z. (1994) *Biochim. Biophys. Acta* 1199, 105–114.
- [27] Kayushina, R.L., Tolstikhina, A.L., Stepina, N.D., Belyaev, V.V., Lapuk, V.A. and Varlamova, E.Y. (2000) *Crystallogr. Rep.* 45, 1001–1006.
- [28] Kim, D.T., Blanch, H.W. and Radk, C.J. (2002) *Langmuir* 18, 5841–5850.
- [29] Chao, H., Martin, G.G., Russel, W.K., Waghela, S.D., Russell, D.H., Schroeder, F. and Kier, A.B. (2002) *Biochemistry* 41, 10540–10553.
- [30] Færgeman, N.J., Sigurskjold, B.W., Kragelund, B.B., Andersen, K.V. and Knudsen, J. (1996) *Biochemistry* 35, 14118–14126.